Agricultural and Forest Meteorology 375 (2025) 110868

Contents lists available at ScienceDirect

Agricultural and Forest Meteorology

journal homepage: www.elsevier.com/locate/agrformet

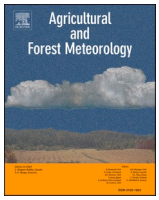

Automatic calibration of the Biome-BGC model with the PEST software to simulate the forest and farmland ecosystems of the Qinling Mountains in China

Kaiyuan Gong [a,b], Zhuo Huang [a,b], Linsen Wu [a,b], Zhihao He [a,b], Junqing Chen [a], Zhao Wang [c], Qiang Yu [c,d], Hao Feng [d], Jianqiang He [a,b,c,*]

[a] Key Laboratory for Agricultural Soil and Water Engineering in Arid Area of Ministry of Education, Northwest A&F University, Yangling, Shaanxi 712100, China
[b] Institute of Water-Saving Agriculture in Arid Areas of China, Northwest A&F University, Yangling, Shaanxi 712100, China
[c] Key Laboratory of Eco-Environment and Meteorology for the Qinling Mountains and Loess Plateau, Shaanxi Provincial Meteorological Bureau, Xi'an, Shaanxi 710015, China
[d] State Key Laboratory of Soil Erosion and Dryland Farming on the Loess Plateau, Institute of Water and Soil Conservation, Northwest A&F University, Yangling, Shaanxi 712100, China

ARTICLE INFO

Keywords:
Biome-BGC model
Parameter estimation
Parameter estimation (PEST)
Gross primary productivity
Evapotranspiration

ABSTRACT

Ecological models are important tools for quantifying and evaluating the carbon and water cycles of agricultural and forest ecosystems. However, quick determination of the values of parameters of a given model remains a big challenge for most model users, especially beginners. In this study, we coupled an independent automatic parameter optimization tool of PEST (Parameter ESTimation) with the Biome-BGC model through Python programming language, and finally developed a new Biome-BGC-PEST software package for automatic model optimization. The encapsulation of the optimization process for Biome-BGC model parameters has heavily simplified model operational steps and improved model calibration efficiency. With the Biome-BGC-PEST package, sensitivity analysis and optimization of physiological and ecological parameters of the Biome-BGC model were conducted based on combined remote-sensing products of GPP (Gross primary productivity) and ET (Evapotranspiration) for the agricultural and forest ecosystems in the Qinling Mountains of China. Compared with the traditional trial-and-error methods for parameter optimization, the influential parameters estimated by the Biome-BGC-PEST package were similar, mainly including atmospheric deposition of N, symbiotic and asymbiotic fixation of N, cuticular conductance, etc. However, they were dramatically different in their sensitivity magnitudes. This was mainly because the new method greatly enhanced the efficiency of parameter optimization through allowing simultaneously tuning all of the parameters related to carbon and water fluxes. Consequently, the simulation accuracy of the Biome-BGC model was dramatically improved for the agricultural and forest ecosystems in the Qinling Mountains after parameter optimization. The R^2 (Coefficient of determination) of general GPP simulations increased from 0.67 to 0.89 and the RMSE (Root mean square error) decreased by about 37 %. Similarly, the R^2 of general ET simulations increased from 0.57 to 0.86 and the RMSE decreased by about 55 %. In conclusion, the newly established Biome-BGC-PEST package demonstrated similar or better optimization efficiency and accuracy compared to the traditional methods, which could greatly promote the application of the Biome-BGC model in relevant research of agricultural and ecological modeling.

1. Introduction

Forest ecosystems store 70 % of the global terrestrial vegetation carbon pool (Ciais et al., 2014) and contribute to half of the global terrestrial carbon sequestration(Beer et al., 2010; Pan et al., 2011). The carbon and water cycles of ecosystems are closely linked to global ecosystem changes. Quantifying and assessing the carbon and water cycles, as well as energy allocation in forest and agricultural ecosystems are of great importance for the studies on regional carbon budgets, water cycles, and climate change at regional scales. This study specifically

* Corresponding author.
E-mail address: jianqiang_he@nwsuaf.edu.cn (J. He).

https://doi.org/10.1016/j.agrformet.2025.110868
Received 25 September 2024; Received in revised form 20 September 2025; Accepted 26 September 2025

focuses on the process of parameter optimization for the Biome-BGC model to improve its performance in simulating forest and agricultural ecosystems. Simultaneously, the water cycle within forest ecosystems constitutes a crucial component of the terrestrial water cycle, governing the dynamic allocation, transportation, and transformation of various forms of water in the forest ecosystems (Liu and Wu, 2012). With the increase of human activities, agricultural production has been influencing the carbon and water cycles of terrestrial ecosystems through alterations in land use patterns, soil, and vegetation structure (Xia et al., 2021).

Studying water-carbon flux usually involves separately measuring the carbon sequestration (in terms of gross primary productivity, GPP) and water consumption components (in terms of evapotranspiration, ET) of terrestrial vegetation (Baldocchi, 1994; Beer et al., 2009). The GPP of an ecosystem refers to the amount of carbon fixed by green plants per unit area over a unit of time through photosynthesis (Wang et al., 2023b; Yu et al., 2023). It serves as the foundation of the ecosystem carbon cycle and represents the initial material and energy acquisition for the ecosystem (Ryu et al., 2011). Evapotranspiration is the sum of vegetation transpiration, soil evaporation, and evaporation intercepted by the canopy. It constitutes a crucial component of both the global water cycle and the Earth's surface energy balance (Priestley and Taylor, 1972; Ryu et al., 2011). Due to the complexity and the temporal and spatial variability of these fluxes, process-based ecosystem models have become essential tools to integrate and extrapolate them to broader spatial scales.

Process-based ecosystem models are research tools constructed on theoretical foundations through mathematical equations. They simulate and predict the mechanisms of the whole ecosystem based on local dynamics, allowing the extrapolation of small-scale carbon and water cycle relationships to larger spatial scales. These models provide an effective approach for investigating the coupled carbon-water relationships at regional scales. The Biome-BGC model could provide accurate descriptions of carbon, nitrogen, and water cycle dynamics in various vegetation types (Running and Hunt Jr, 1993). Among the many process-based ecosystem models available, the Biome-BGC model stands out for its detailed representation of vegetation physiological processes, more comprehensive simulation over time, and higher level of integration. However, a major challenge in the current applications of the Biome-BGC model lies in the sensitivity analysis and optimization of model parameter. Once optimized and validated, the model can be widely used in the simulations and analyses of carbon and water fluxes across diverse ecosystems including forests, grasslands, and agricultural fields (Bond-Lamberty et al., 2007; Ren et al., 2022; Sun et al., 2017).

Currently, methods used for sensitivity analysis of model parameters mainly included local sensitivity analysis (Kumar and Raghubanshi, 2012) and global sensitivity analysis (Raj et al., 2014; Yan et al., 2016). The method for model parameter estimation usually involved referencing parameter values from previous studies and refining them with physiological principles of plants. Influential model parameters were continuously adjusted within a reasonable range, and parameter values were ultimately determined for various natural vegetation types (Chen and Xiao, 2019; Ren et al., 2022; Ueyama et al., 2010). These methods have been widely applied in previous studies related to the Biome-BGC model. However, they suffer from issues such as low parameter optimization efficiency, high entry barriers, and significant uncertainties in optimization results, with the parameter optimization process typically occupying most of the time in these studies (Huang et al., 2022a; Jia and Zhang, 2024; Liu et al., 2025; You et al., 2019). Therefore, this study aims to improve the efficiency and accuracy of parameter optimization for the Biome-BGC model using parameter optimization software. The PEST (Parameter ESTimation) is a nonlinear parameter estimation software widely used for the automatic estimation of parameters in almost any kind of computer models (Friedel, 2005).

PEST adjusts model parameters based on multiple model runs until the model output closely matches the observed values. PEST utilizes the

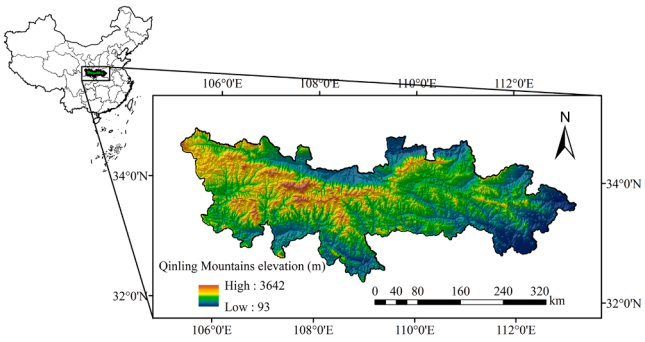

Fig. 1. Location and elevation map of the Qinling Mountains of China.

Gauss-Marquardt-Levenberg (GML) algorithm, which is a gradient-based method, to optimize model parameters. The theoretical foundation of the GML method stems from linear parameter estimation theory. The GML algorithm enhances the ability to identify the global minimum for the model (Skahill and Doherty, 2006). The most remarkable advantage of the GML method is its ability to achieve parameter estimation with very high model efficiency (Ma et al., 2020). In recent years, the PEST software has been widely used hydrological models, crop models, and physiological-ecological models, demonstrating favorable parameter optimization performance in these models (Bahremand and De Smedt, 2010; Bezak et al., 2015; Gao et al., 2014; Ma et al., 2012; Tebakari and Kita, 2015). However, due to the difficulty of getting started and the cumbersome operation of the PEST software, its application in the Biome-BGC model was very limited. In PEST optimization, manual adjustment of parameter ranges is required for each round of optimization, which consumes a considerable amount of time and leads to low efficiency. PEST application requires a professional programmer to write computer code, prepare relevant files, and invoke PEST running within the model. This kind of programming demand may pose a great challenge for model users, especially the beginners (Fang et al., 2010).

To address this issue, this study coupled the Biome-BGC model with the PEST software. The main objectives were to (1) encapsulate the parameter optimization steps of the PEST software into the Biome-BGC model for automatic model calibration; (2) assess the applicability of calibrated Biome-BGC model in simulating the forest and farmland ecosystems of the Qinling Mountains; and (3) propose a replicable model calibration approach for regional-scale applications of the Biome-BGC model.

2. Materials and methods

2.1. Study area

The Qinling Mountains is a geographical dividing line between northern China and southern parts of China, running in a west-to-east direction and spanning across Gansu Province, Shaanxi Province, and Henan Province. The Qinling Mountains are located at an east-west distance of 1600 km and a north-south distance of 100–300 km, with elevations of 95–3881 m (Fig. 1). The Qinling Mountains serve as the boundary between the subtropical and the warm temperate climates in China. It is bordered by the Weihe River to the north and the Hanjiang River to the south. The region has abundant precipitation, with an annual average of 600–1200 mm. However, there are considerable variations in seasonal rainfall distributions. The obvious climatic difference between the northern and southern slopes can be attributed to the pronounced obstruction of mountain ranges to atmospheric flow. The northern slope belongs to a warm-temperate, semi-humid climate, characterized by an annual average precipitation of 520 mm and an annual average temperature of 10 °C. In contrast, the southern slope falls within the subtropical, humid climate zone, with an annual average

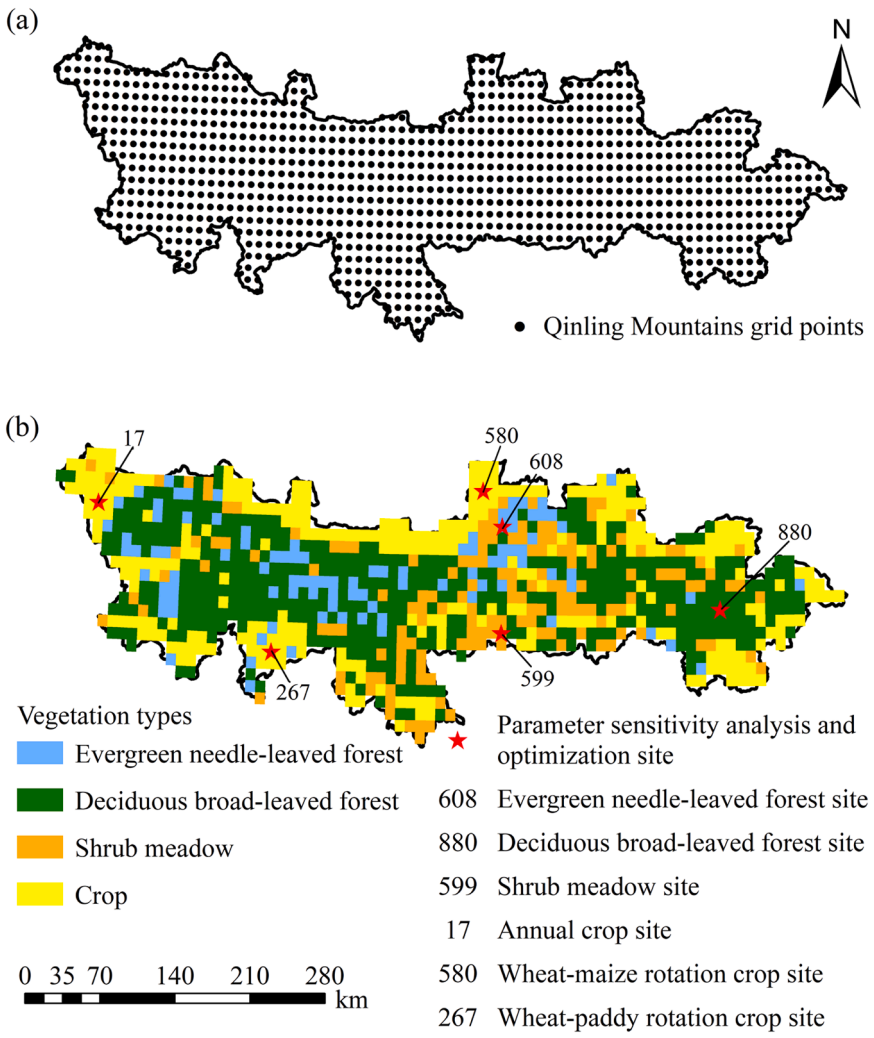

Fig. 2. Schematic diagram of the distribution of grid points (a) and the four typical vegetation types (b) in the Qinling Mountains of China. Arabic numbers of 17, 267, 580, 599, 608, and 880 indicate the six selected representative sites of typical vegetation types for sensitivity analysis of the parameters of Biome-BGC model.

precipitation of 820 mm and an annual average temperature of 14 °C (Wang and Bai, 2017). The Qinling Mountains are characterized by abundant vegetation, high forest coverage, well-defined vertical zonation spectrum of vegetations, and exceptionally rich biodiversity. The region encompasses various vegetation types, including deciduous broad-leaved forests, evergreen coniferous forests, mixed conifer-broadleaved forests, as well as subalpine meadows, alpine grasslands, shrublands, and farmlands. Therefore, it holds significant importance to study on the ecosystem of the Qinling Mountains to address the issues related to water conservation and ecological protection.

2.2. Brief introduction to the Biome-BGC model

The Biome-BGC model is a typical process-based terrestrial ecosystem model that simulates the water, carbon, oxygen cycles, as well as energy flow within vegetation, litter, and soil components of terrestrial ecosystems. The Biome-BGC model was jointly developed and maintained by the National Center for Atmospheric Research (NCAR) and the Numerical Terradynamic Simulation Group (NTSG) at the University of Montana, United States. Since the initial release of the first-generation Biome-BGC model in 1993, the running team has continuously worked on improving and enhancing the model to refine the carbon, water, and nutrient cycling and storage processes within the atmosphere-vegetation-soil interactions of terrestrial ecosystems (Running and Hunt Jr, 1993). The current version of the Biome-BGC model is V4.2 (https://www.ntsg.umt.edu/project/biome-bgc.php), which comprehensively considers the carbon, nitrogen, and water cycles, as well as soil processes and energy flows within ecosystem processes. It has become a widely recognized ecological process simulation model in the forefront of international researches (Chiesi et al., 2007; Li et al., 2020; White et al., 2000).

2.3. PEST software

The PEST software is parameter-independent and uncertainty-analysis-based software (Doherty et al.). PEST is also a parameter estimation tool renowned for its ability to optimize model parameters without requiring any modifications to the original model structure. This exceptional characteristic endows PEST with robust adaptability, enabling seamless integration with a wide range of existing models (Fang et al., 2012; Nolan et al., 2010; Zhen et al., 2023). By incorporating PEST into a given model, it can be transformed to a non-linear parameter estimator or a sophisticated data interpretation package for the model simulation system. The main algorithm of PEST estimates model parameters by minimizing a given objective function. The objective function, denoted as $\psi(F)$, is defined as a weighted least-squares difference function based on the observed and calculated values of one or multiple output variables with respect to the model parameters (Eq. (1)). In this study, observations of GPP and ET fluxes

were employed as input data. The PEST software was utilized to perform the optimization for the Biome-BGC model.

$$\psi(F) = \psi_{(GPP)} + \psi_{(ET)} = \sum_{i=1}^{n_1} w_{GPP,i}^2 \left(obs_{GPP,i} - sim_{GPP,i}\right)^2 + \sum_{i=1}^{n_2} w_{ET,i}^2 \left(obs_{ET,i} - sim_{ET,i}\right)^2 \quad (1)$$

where $\psi(F)$ represents the objective function; the subscript GPP indicates gross primary productivity; the subscript ET denotes evapotranspiration; *obs* refers to the observed values; *w* represents the weight coefficient assigned to each observed value; *sim* represents the simulated values; *i* denotes the time step ($i = 1$ to 365, representing the daily time steps for the Biome-BGC model); and n_1, n_2 denote the number of observed values for GPP and ET, respectively. In this study, there are observed flux data for 365 days in each year.

The PEST software requires three types of input files: (1) the template files, in which model input files and the parameters are identified; (2) instruction files, in which identifies the templates and output data; and (3) a control file, which controls the PEST optimization process. Once built, these files can be checked for correctness and consistency by

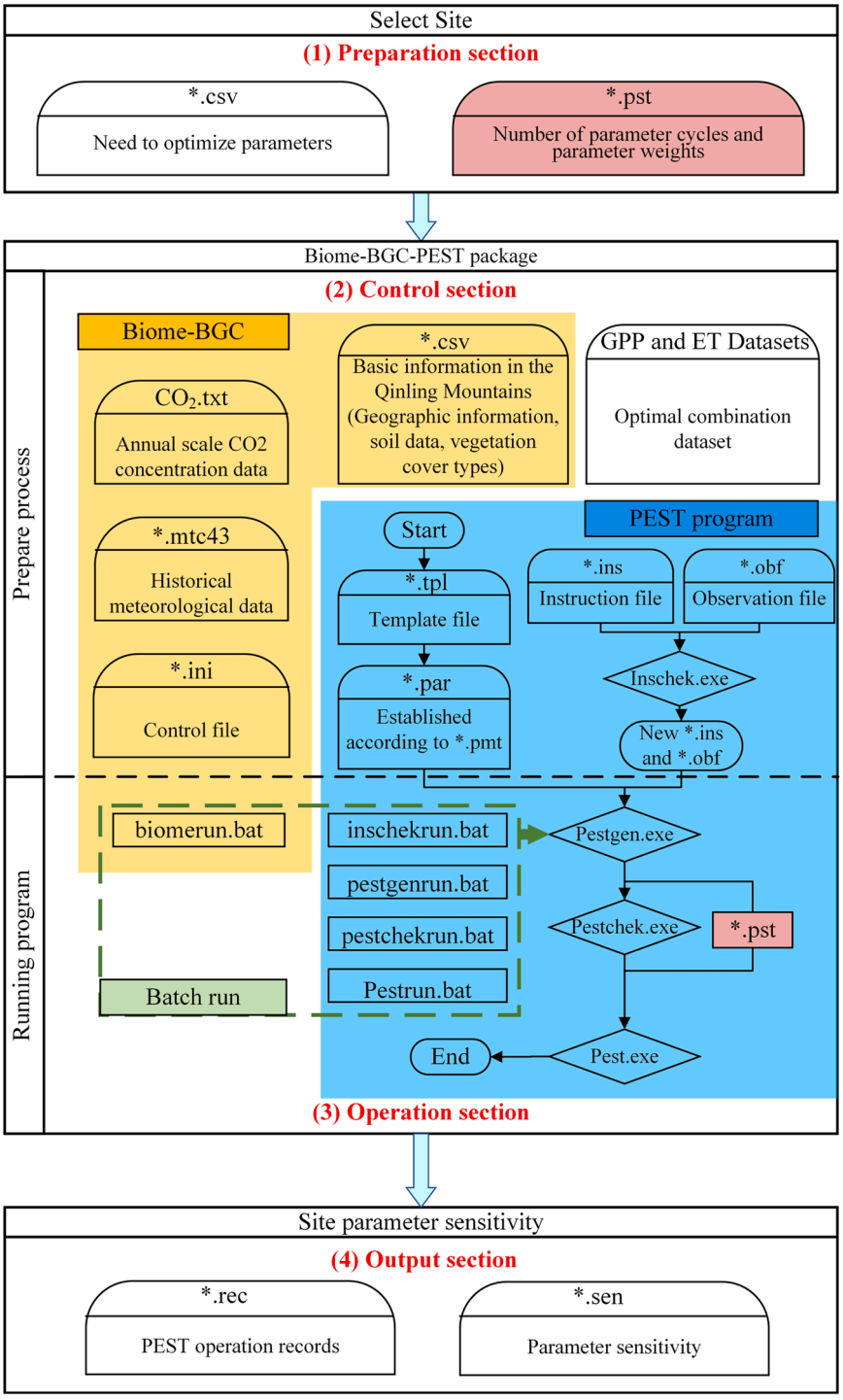

Fig. 3. Flowchart of the automatic parameter optimization process for the Biome-BGC-PEST package. Blue part indicates the running process of the PEST software program; yellow part indicates the running process of the Biome-BGC model; and green part the batch running program that couples the PEST and the Biome-BGC.

the programs of TEMPCHEK, INSCHEK, and PESTCHEK (Malone et al., 2010; Nolan et al., 2010). In the application of PEST, it is essential for users to ensure the successful execution of the target model before preparing PEST files. Subsequently, correct commands should be written in Windows DOS command line mode to validate the files and run the PEST program.

2.4. Data acquisition and processing

2.4.1. Data for Biome-BGC model simulation

Primary data utilized in this study include climate, vegetation cover, soil, DEM (digital elevation model), and other foundational geographical information data. Meteorological data of 2003-2016 were obtained from the National Tibetan Plateau Data Center (http://westdc.westgis.ac.cn/). This dataset encompassed daily maximum and minimum temperatures (°C) as well as daily precipitation (mm). To provide complete meteorological data necessary for the Biome-BGC model running, the Mountain Microclimate Simulation Model (MT-CLIM) was employed to generate the meteorological data required (Running et al., 1987). The MT-CLIM model was utilized to estimate site-level daily values of various climatic variables, including solar radiation, vapor pressure deficit, and daylength based on the observed data of daily maximum temperature, minimum temperature, and precipitation. Vegetation cover data were obtained from the National Tibetan Plateau Data Center (https://www.ncdc.ac.cn/). The dataset utilized in this study was the Chinese Vegetation Functional Type map, with a spatial resolution of 1 km (Hengl et al., 2014). The soil data were obtained from the Global Soil Information System (https://soilgrids.org/). This system provides soil grid data at a spatial resolution of 1 km. The dataset includes various soil attributes such as soil organic carbon content (g kg^{-1}), pH, bulk density (kg m^{-3}), coarse fraction (%), soil organic carbon stock (t ha^{-1}), rock depth (cm), as well as the composition of sand, silt, and clay components (%). Elevation data were sourced from the Shuttle Radar Topography Mission (SRTM)(Farr and Kobrick, 2000), while the other fundamental geographical data included site latitude information.

2.4.2. Data rasterization

In this study, the Qinling Mountains was partitioned into fundamental spatial units. These units were simulated individually, enabling the regionalized running of the model. Specifically, the Qinling Mountains were divided into 967 grid cells, each with dimensions of 10 km × 10 km (Fig. 2a). The vegetation cover type for each 10 km-resolution grids was determined based on the dominant vegetation type in the grid, which refers to the vegetation type with the largest coverage area within the given grid. Furthermore, the diverse multi-dimensional data required for the operation of the Biome-BGC model were harmonized to a consistent resolution.

2.4.3. Validation data of GPP and ET preparation

To verify model simulation accuracy, it is essential to compare model simulations with the corresponding observations of GPP and ET for different vegetation cover types in the Qinling Mountains. The accuracy of different satellite remote-sensing products could vary heavily for different vegetation cover types. Therefore, this study referred to previous research findings and selected the most accurate products available in China for each of the four vegetation cover types in the Qinling Mountains (Table S1) (Huang et al., 2022b). Subsequently, the data were standardized to a spatial resolution of 10 km and a temporal resolution of month (30 d). Then, guided by the distributions of vegetation cover in the Qinling Mountains, GPP and ET products were systematically integrated grid by grid for the four different vegetation cover types. Finally, optimized composite datasets of GPP and ET were provided for the Qinling Mountains. More details about the producing process of GPP and ET composite products could be found in Huang et al. (2022b). This study selected the composite datasets of GPP and ET of 2003–2016 as observational data for future analysis (Fig. 2b).

2.4.4. Statistical analysis

This study evaluated the optimization results of the Biome-BGC model and assessed the model's regional adaptability according to two statistical metrics: the coefficient of determination (R^2; Eq. (2)) and the root mean square error (RMSE; Eq. (3)). Meanwhile, to calculate the systematic trend changes in the model optimization results, we also computed the mean bias error (MBE; Eq. (4)) for different vegetation types.

$$R^2 = \left(\frac{n(\sum xy) - (\sum x)(\sum y)}{\left[n\sum x^2 - (\sum x)^2 \right] \left[n\sum y^2 - (\sum y)^2 \right]} \right)^2 \quad (2)$$

$$\mathrm{RMSE} = \left[\left(\sum (x-y)^2 \Big/ n \right) \right]^{0.5} \quad (3)$$

$$\mathrm{MBE} = \frac{\sum x - y}{n} \quad (4)$$

where x and y represent the simulated and observed values; and n represents the number of paired values. R^2 close to 1 and RMSE, MBE close to 0 indicate a good agreement between model simulations and field observations.

2.5. Biome-BGC and PEST coupling

2.5.1. Establishment of the Biome-BGC-pest package

The PEST software was encapsulated to facilitate the steps and procedures of parameter optimization for the Biome-BGC model. The automatic optimization of model parameters could thereby obviously reduce the errors and improve the efficiency of model calibration. Thus, the Biome-BGC-PEST package was developed with Python language to enable the model integration. The Biome-BGC-PEST package consists of four main components. (1) First, it prepared basic information files (.csv) about parameter optimization sites and control files (.pst) for the PEST program. (2) Next, it started an automatic process wherein the Python program generated files (.ini) related to the Biome-BGC model and the files (*.tpl, *.par, *.pmt, *.ins, *.obf) relevant to the PEST program. (3) Third, the program automatically created commands to write and execute the *.bat files. (4) Finally, these files enable the Biome-BGC-PEST to run automatically and output results (Fig. 3). The Python code and file instructions for the Biome-BGC-PEST package can be found in the supplementary file (Table S2).

To use the Biome-BGC-PEST package, it needed geographic information, land cover data, meteorological data of 2003-2016, and the composite datasets of GPP and ET for the 967 grid points within the Qinling Mountains. Then, researchers can simply select the representative pixels, specify the parameters to be adjusted, and control the files to achieve automatic parameter optimization. In this study, the automatic optimization process of Biome-BGC-PEST package was based on the Monte Carlo method, which generated multiple sets of initial parameter sets within predefined parameter value ranges (set empirically). The initial parameter sets were then utilized to drive the coupled Biome-BGC and PEST program for sequential optimization. The optimization results from all initial parameter sets were collected, but only the parameter set with the best optimization performance was selected as the final optimization result. The number of initial parameter sets can be set in the control file of the package, which was set to 500 sets in this study. This approach could help avoid the problems encountered in some previous studies, in which parameter estimations with the PEST software were only based on a single set of default parameters and the optimization result was easy to be trapped in local optima.

2.5.2. Parameter sensitivity analysis based on the Biome-BGC-pest package

Sensitivity analysis of model parameters was performed using the Biome-BGC-PEST package when simulating typical vegetation types in the Qinling Mountains, including deciduous broad-leaved forests,

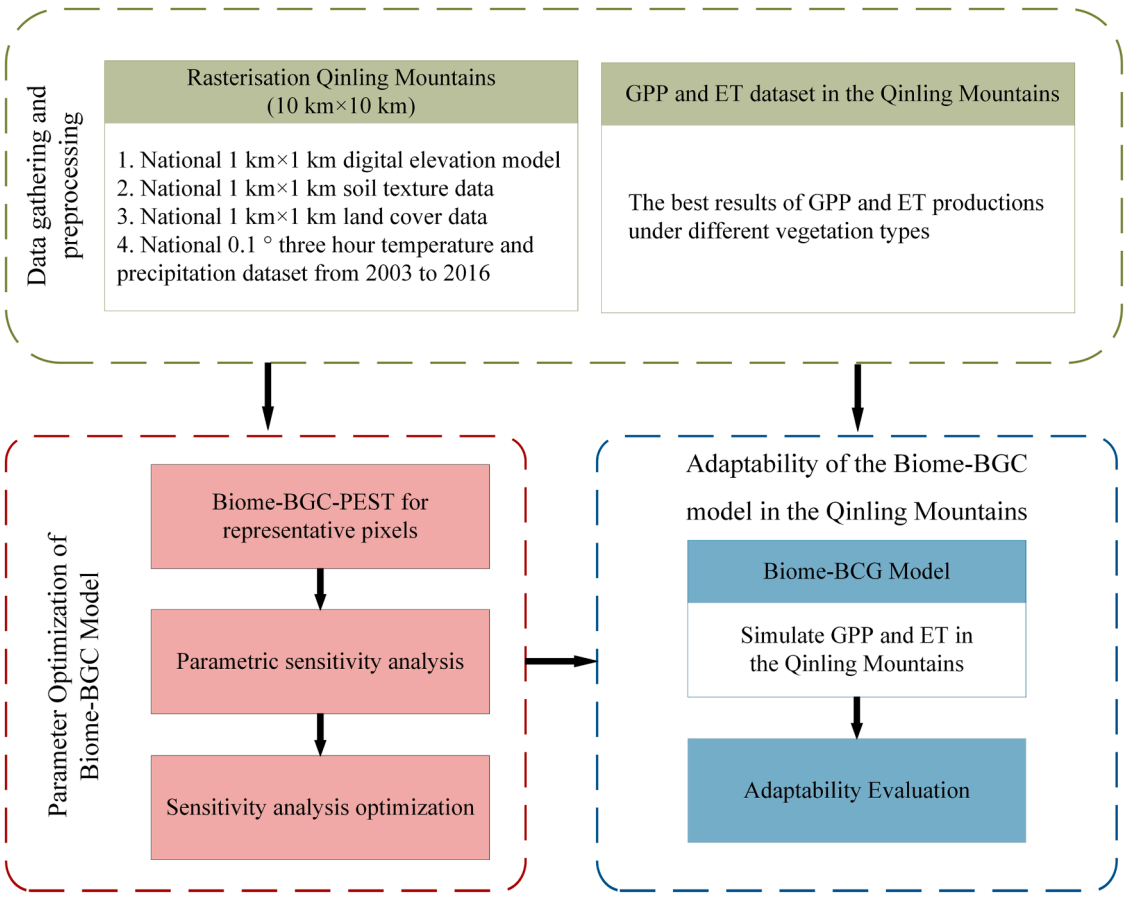

Fig. 4. Flow chart for the adaptability evaluation of the Biome-BGC-PEST package to optimize the parameters of the Biome-BGC model in the Qinling Mountains of China.

evergreen needle-leaved forests, shrub meadows, and crop farmlands. Notably, the crops in the Qinling Mountains exhibited distinct differences compared to the other vegetation types. Based on their cultivation practices, the crops in the study area were categorized into three main types: (1) annual crop (wheat) with one harvest per year, distributed in the northwestern part of the Qinling Mountains; (2) wheat-paddy rotation with two harvests per year, distributed in the southern part of the Qinling Mountains; (3) wheat-maize rotation with two harvests per year, distributed in the northern, eastern, and southern parts of the Qinling Mountains. Hence, for the crop farmlands, separate sensitivity analyses and optimizations of model parameters were conducted for each of the three different cultivation types of annual crop, wheat-maize rotation (where wheat and maize were analyzed separately), and wheat-paddy rotation.

The Biome-BGC model has a total of 43 physiological and ecological parameters, among which the identity-related parameters (e.g., parameter indicating deciduous or herbaceous vegetation) were excluded from the optimization process according to some previous studies. In addition to the physiological ecological parameters, this study added two environmental parameters related to GPP and ET simulations: atmospheric nitrogen deposition and symbiotic and non-symbiotic nitrogen. Therefore, there were a total of 41 parameters (Table S3). The Biome-BGC-PEST package was applied separately using the initial parameter files provided by the model for different vegetation types, namely '*enf.epc*' for evergreen needle-leaved forests, '*dbf.epc*' for deciduous broad-leaved forests, '*C3grass.epc*' for wheat, '*C4grass.epc*' for maize, and '*shrub.epc*' for shrub meadows. The initial parameter files of '*C3grass.epc*' (wheat) and '*C4grass.epc*' (maize) were slightly modified based on previous research to better meet the physiological status of the crops (Wang et al., 2005). For each vegetation cover type, random sampling was performed to select the representative sites for sensitivity analysis and optimization of model parameter (Fig. 2b).

Based on the sensitivity analysis files (*.sen) and referring to the manual of the PEST software (Fig. 3), this study set the sensitivity thresholds as 1.0 for forest types (Deciduous broad-leaved forest, evergreen needle-leaved forest, and shrub meadow), and 0.1 for crop types (Annual crop, wheat in wheat-maize rotation, maize in wheat-maize rotation, and wheat-paddy rotation). After the program was run, the influential parameters of each vegetation type were obtained according to the sensitivity values to GPP and ET (Fig. 4). The sensitivity analysis files (*. sen) is based on the calculation of Jacobian matrices in the PEST optimization process (Doherty et al.). Based on the contents of the Jacobian matrix, PEST calculates the composite sensitivity of *i* th parameter with respect to all observations (Eq. (5)).

$$s_i = \frac{(J^t Q J)_{ii}^{1/2}}{m} \tag{5}$$

where s_i is the comprehensive sensitivity of the *i* th parameter; *J* is the Jacobian matrix; *Q* is the cofactor matrix; and *m* is the weighted average of the observed values. Thus, the composite sensitivity of the *i* th parameter is the normalized (with respect to the number of observations) magnitude of the column of the Jacobian matrix pertaining to that parameter, with each element of that column multiplied by the weight pertaining to the respective observation.

2.5.3. Optimization of influential model parameters

The composite datasets of GPP and ET were utilized as observations at the selected sites in the Qinling Mountains (Fig. 4). Data in 2003-2012 were employed for parameter optimization, while data in 2013-2016

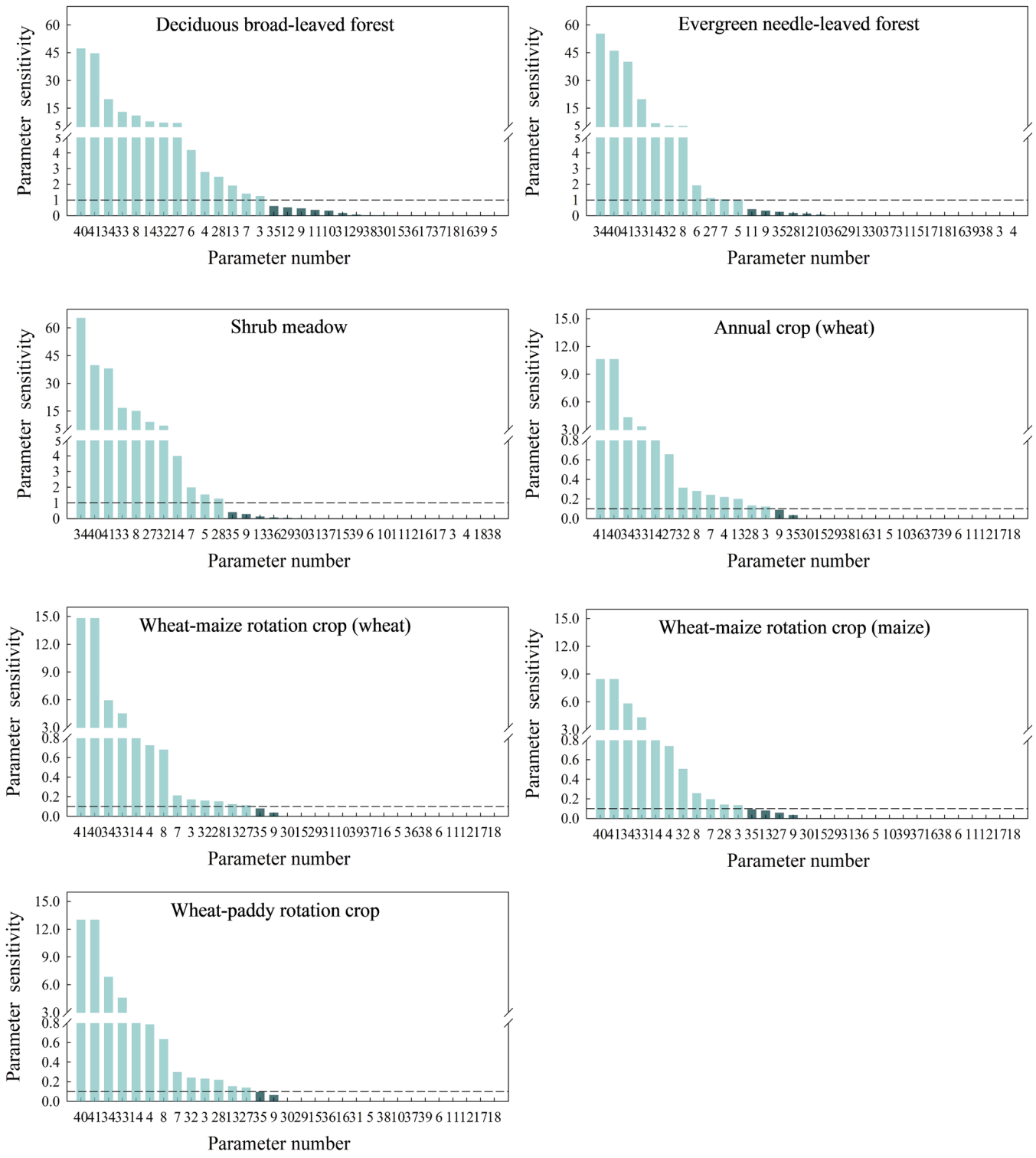

Fig. 5. Histogram of parameter sensitivities in the simulations of GPP and ET with the Biome-BGC model under typical vegetation types (deciduous broad-leaved forest, a; evergreen needle-leaved forest, b; shrub meadow, c; annual crop, d; wheat in wheat-maize rotation, e; maize in wheat-maize rotation, f; and wheat-paddy rotation, g) in the Qinling Mountains of China. The parameters with sensitivities above the dotted lines are selected as the influential parameters.

were reserved for model validation. The optimization of influential parameter was conducted with the Biome-BGC-PEST package for typical vegetation types (i.e., deciduous broad-leaved forests, evergreen needle-leaved forests, shrub meadows, and crop farmlands of annual crop, wheat-maize rotation, and wheat-paddy rotation) (Table S4) in the Qinling Mountains. In the wheat-maize rotation system, parameters for wheat and maize were optimized separately. To achieve separate optimizations for wheat and maize at the grids of wheat-maize rotation, the weights of observations were adjusted according to the growth months of wheat and maize. The simulated variable values of wheat and maize were combined based on the weights for model validation and evaluation.

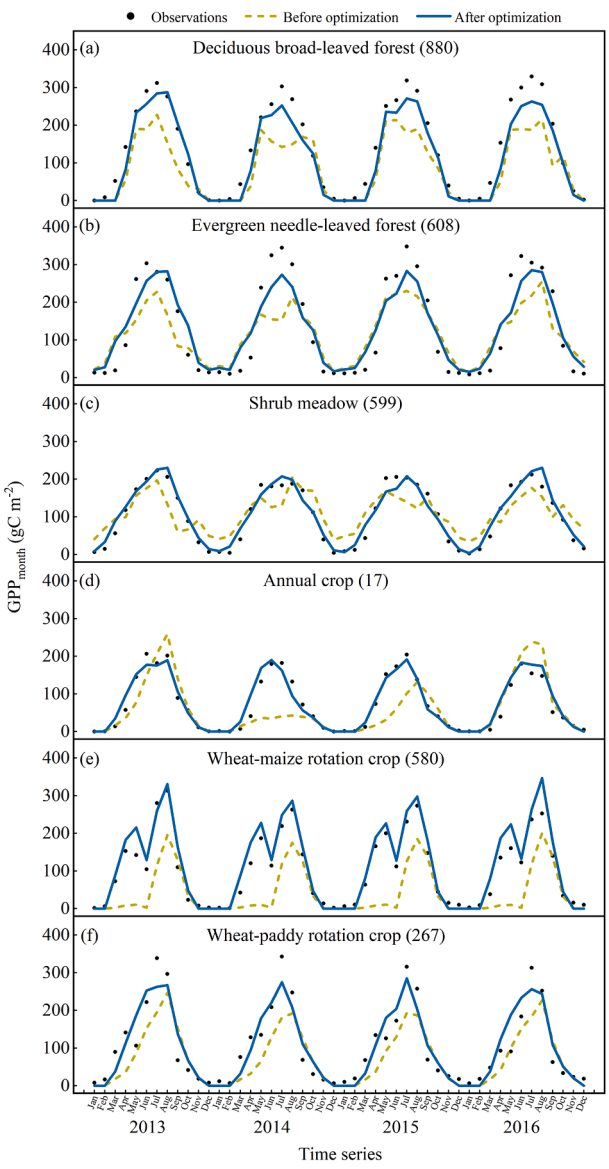

Fig. 6. Comparisons of observed and simulated GPP$_{month}$ with the Biome-BGC model before (green dashed lines) and after (blue solid lines) the optimization of influential parameters of the Biome-BGC model under different typical vegetation cover types (deciduous broad-leaved forest, a; evergreen needle-leaved forest, b; shrub meadow, c; annual crop, d; wheat-maize rotation, e; and wheat-paddy rotation, f) in the Qinling Mountains of China. The numbers in the parentheses after vegetation types are the representative site number as shown in Fig. 2. And the same below.

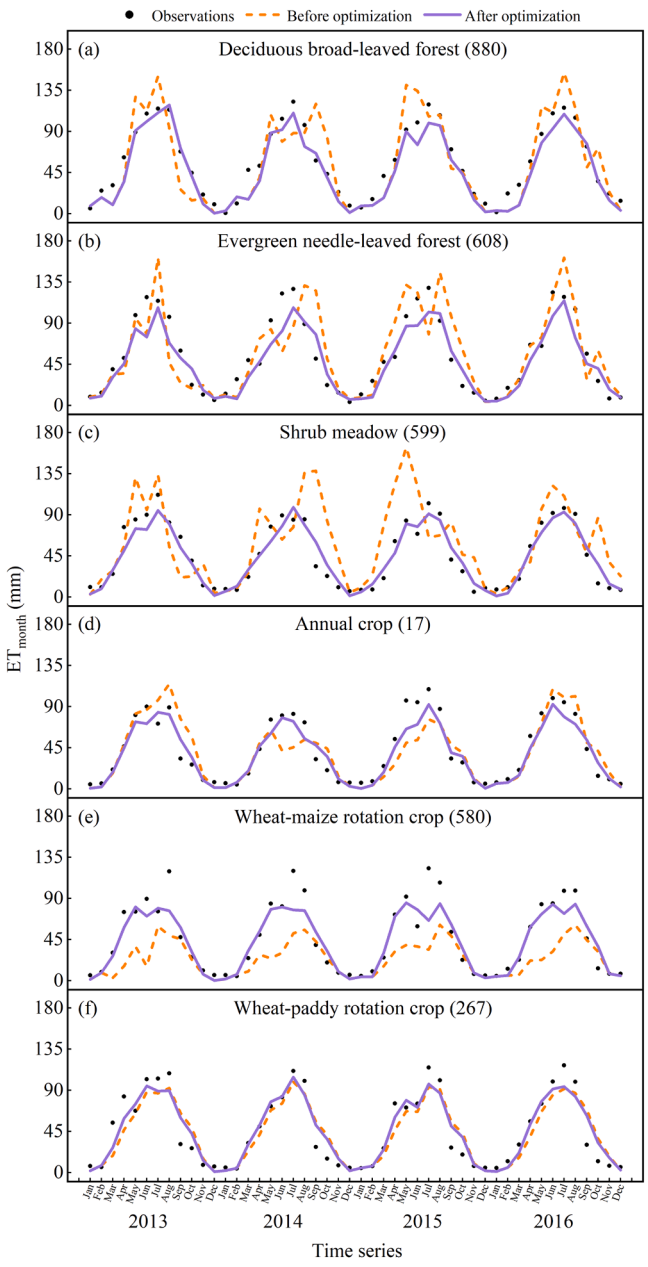

Fig. 7. Comparisons of observed and simulated ET$_{month}$ with the Biome-BGC model before (red dashed lines) and after (violet solid lines) the optimization of influential parameters of the Biome-BGC model under different typical vegetation cover types (deciduous broad-leaved forest, a; evergreen needle-leaved forest, b; shrub meadow, c; annual crop, d; wheat-maize rotation, e; and wheat-paddy rotation, f) in the Qinling Mountains of China.

3. Results

3.1. Model parameter optimization with the Biome-BGC-pest package

3.1.1. Parameter sensitivity analysis

Sensitivities of different parameters of the Biome-BGC model were obtained for each coverage type by optimizing model parameters at different sites with various vegetation covers. This process allowed us to select the most influential parameters. The results of sensitivity analysis revealed that there were a total of 14 influential parameters for the GPP and ET simulations of deciduous broad-leaved forest, while evergreen needle-leaved forest and shrub meadow both only had 11 influential parameters (Fig. 5). For crops, the number of influential parameters was 11 for the maize in the wheat-maize rotation, while it was thirteen for the other crop types. The most influential parameters across all vegetation cover types were the “atmospheric deposition of N”, “symbiotic and asymbiotic fixation of N”, “cuticular conductance”, and “maximum stomatal conductance”. The influential parameters were summarized for typical vegetation types for GPP and ET simulations in the Qinling Mountains (Tables S5 and S6). It was found that the types of influential parameters were very similar across different vegetation cover types.

3.1.2. Optimization of influential parameters for different vegetation cover types

Before parameter optimization, the model performance in GPP$_{month}$ simulations for deciduous broad-leaved forest (Fig. 6a), evergreen needle-leaved forest (Fig. 6b), shrub meadow (Fig. 6c), and paddy-

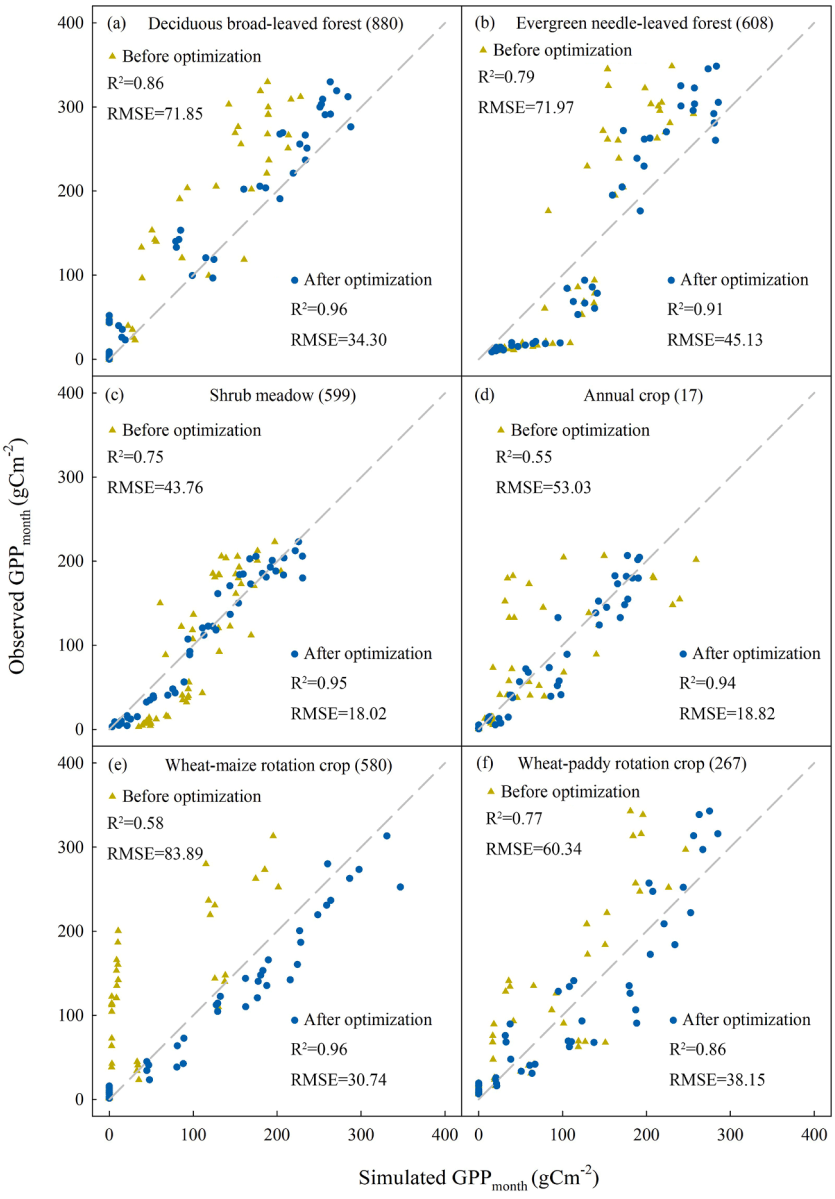

Fig. 8. Scatter plots of observed and simulated GPP_{month} with the Biome-BGC model before (green triangles) and after (blue dots) parameter optimization under typical vegetation cover types (deciduous broad-leaved forest, a; evergreen needle-leaved forest, b; shrub meadow, c; annual crop, d; wheat-maize rotation, e; and wheat-paddy rotation, f) in the Qinling Mountains of China.

wheat rotation crop (Fig. 6f) was better than that for annual crop (Fig. 6d) and wheat-maize rotation (Fig. 6e). Particularly at the grids of wheat-maize rotation, there was a notable variation in GPP_{month} before and after the rotation. This phenomenon could be attributed to the lack of model parameter optimization, which consequently hindered an accurate representation of the GPP_{month} fluctuations. As a result, remarkable disparities between simulated and observed values were observed. The simulation results of ET_{month} before optimization showed that the wheat-paddy rotation (Fig. 7f) grids exhibited the most favorable simulation performance, while the simulations at shrub meadow (Fig. 7c) and wheat-maize rotation grids (Fig. 7e) showed substantial discrepancies compared to the observed values. However, the simulation performance of GPP_{month} and ET_{month} was generally improved to varying degrees for all vegetation cover types after model parameter optimization. At the grids of wheat-maize rotation, separately optimized parameters for wheat and maize could help capture the changes in GPP_{month} before and after rotation, resulting in an obvious enhancement of simulation accuracy. The simulated values generally became much close to the observed values and shared similar temporal variation patterns.

The GPP_{month} and ET_{month} simulation results with the Biome-BGC model were compared before and after parameter optimization across different vegetation cover grids based on the statistics of R^2 and RMSE. After model parameter optimization, the R^2 of GPP simulation increased from 0.86 to 0.96 at deciduous broad-leaved forest grids, and RMSE decreased from 71.84 gC m^{-2} to 34.30 gC m^{-2}. At evergreen needle-leaved forest grids, the R^2 of GPP_{month} simulation increased from 0.79 to 0.91, while RMSE decreased from 71.97 gC m^{-2} to 45.13 gC m^{-2}. For shrub meadow grids, the R^2 and RMSE after parameter optimization were 0.95 and 18.02 gC m^{-2}, respectively. Similarly, for the GPP_{month} simulations at the three crop grids, it demonstrated that the Biome-BGC model generally had increased R^2 and reduced RMSE values after model parameter optimization (Fig. 8). The ET simulation accuracy of the Biome-BGC model was also greatly enhanced after parameter optimization. The shrub meadow grids had the lowest R^2 (0.49) before parameter optimization, but achieved an R^2 of 0.92 after parameter

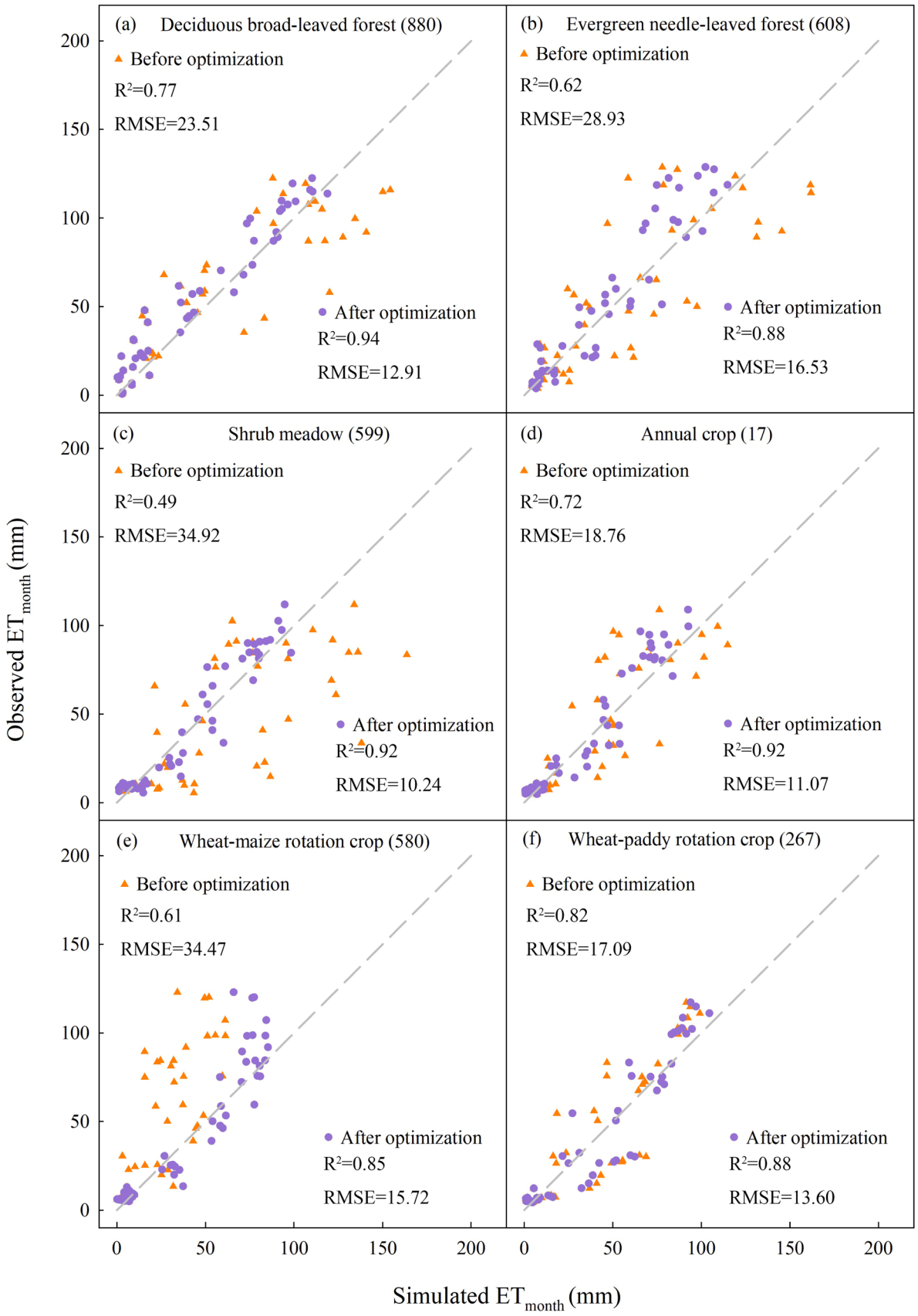

Fig. 9. Scatter plots of observed and simulated ET_{month} with the Biome-BGC model before (orange triangles) and after (violet dots) parameter optimization of typical vegetation cover types (deciduous broad-leaved forest, a; evergreen needle-leaved forest, b; shrub meadow, c; annual crop, d; wheat-maize rotation, e; and wheat-paddy rotation, f) in the Qinling Mountains of China.

Table 1
Statistics of R^2, RMSE and MBE between simulated and observed GPP_{month} before and after optimization of the Biome-BGC model parameters under different vegetation cover types of the Qinling Mountains of China.

Vegetation type	Before parameter optimization			After parameter optimization		
	R^2	RMSE (gC m^{-2})	MBE (gC m^{-2})	R^2	RMSE (gC m^{-2})	MBE (gC m^{-2})
Deciduous broad-leaved forest	0.78	70.91	−25.75	0.93	46.70	−10.12
Evergreen needle-leaved forest	0.59	78.16	−10.10	0.87	56.86	5.52
Shrub meadow	0.73	53.05	1.96	0.94	33.28	−0.15
Annual crop	0.62	76.54	−14.95	0.89	56.74	2.66
Wheat-maize rotation crop	0.38	104.02	−61.77	0.79	56.23	11.64
Wheat-paddy rotation crop	0.74	81.83	−30.57	0.91	47.05	−2.08
The Qinling Mountains	0.67	75.99	−23.53	0.89	47.86	1.24

optimization. Similarly, for all vegetation cover types, the R^2 values were consistently above 0.85 after parameter optimization. Scatter plots of simulation results revealed a substantial enhancement of R^2 values after model parameter optimization, predominantly exceeding 0.9. The reductions of RMSE values were between 20 % and 60 %, with an average decrease of 40 % (Fig. 9).

In general, the simulated GPP and ET curves by the Biome-BGC model with the optimized model parameters were much closer to the observations than those with parameters without optimization. This kind of model performance improvement was evident based on the substantial increase in R^2 and decrease in RMSE values, indicating that the optimized parameters could help better capture the variations in GPP_{month} and ET_{month}, leading to enhanced simulation accuracies.

3.2. Performance of calibrated Biome-BGC model in the Qinling Mountains

3.2.1. GPP simulation performance

The calibrated Biome-BGC model was then used to simulate GPP and ET under different vegetation cover types of the Qinling Mountains of China. Based on the statistics of R^2 and RMSE between observed and simulated values of variables concerned in years of 2003-2016, the adaptability of the Biome-BGC model was evaluated for the simulations of ecosystems in the Qinling Mountains. Generally, simulation performance for GPP in forest types was better than that for crops before parameter optimization (Table 1). However, through parameter optimization, the R^2 values generally increased for all vegetation cover types, and the RMSE values decreased to varying degrees, indicating reduced discrepancies between observations and model simulations under different vegetation cover types. By comparing the differences in MBE before and after parameter optimization, we found that the simulation results for all vegetation types except shrub meadows generally underestimated GPP prior to optimization. Parameter optimization has enabled the simulation results of GPP in the Qinling Mountains to be closer to the actual values. Overall, compared to the model performance before parameter optimization, the performance of Biome-BGC model for GPP simulation improved remarkably in the Qinling Mountains, with an increase of average R^2 from 0.67 to 0.89 and a decrease of average RMSE from 75.99 to 47.86 gC m^{-2} in the entire region.

Through the Taylor diagrams, obvious differences in the distributions of scatter points were observed before and after model parameter optimization (Fig. 10). Before optimization, R^2 values ranged between 0.2 and 0.8 for different cover types, while RMSE values ranged between 40 and 150 gC m^{-2}. Among these vegetation cover types, deciduous broad-leaved forest (Fig. 10a) and shrub meadow (Fig. 10e) exhibited better simulation performance than the other vegetation cover types, while regions with wheat-maize rotation showed the poorest performance. After optimization, R^2 values concentrated between 0.8 and 0.95 and RMSE values ranged from 15 to 90 gC m^{-2}. Compared to the results before optimization, R^2 values became higher, RMSE values became lower, and scatter points were more concentrated. Notably, the improvement in simulation performance was most obvious in regions of wheat-maize rotation (Fig. 10e). Combining the Taylor diagrams (Fig. 10) with the vegetation distributions in the Qinling Mountains (Fig. 2b), it was observed that deciduous broad-leaved forest and shrub meadow regions were interconnected and their scatter points in Taylor diagram were relatively concentrated. Conversely, crop planting regions were scattered along the edges of the entire Qinling Mountains and had more dispersed scatter points in Taylor diagram. This indicates that the original parameters of forest ecosystems (Deciduous broad-leaved forest, Evergreen needle-leaved forest, Shrub meadow) are relatively good, with a small improvement after optimization, while farmland ecosystems, especially those under crop rotation conditions, have a poor simulation basis, so the improvement effect after optimization is the most significant. This is mainly due to the complexity of the farmland ecosystem's own structure and human intervention activities. This indicated that the simulation performance of the Biome-BGC model for GPP was influenced by vegetation cover types and the underlying surface conditions.

According to the distributions of R^2 and RMSE values for GPP simulations across the entire Qinling Mountains (Fig. 11), it was found that R^2 improved from an overall range of 0.6–0.8 to 0.8–1.0, while RMSE decreased from 50–100 gC m^{-2} to 25–75 gC m^{-2} after model parameter optimization. The distributions of R^2 and RMSE before optimization were uneven across the entire area (Fig. 11a and 11c), with overall lower R^2 and higher RMSE values in crop regions. This suggested that the Biome-BGC model had poor performance in simulating GPP for crops, especially for rotation crops. However, the Biome-BGC model had a dramatic improvement in the simulation of crop GPP after parameter optimization (Fig. 11b and Fig. 11d). The differences of R^2 and RMSE between different grids decreased, resulting in more uniform distributions of R^2 and RMSE across the entire region.

3.2.2. ET simulation performance

Different from the simulation results for GPP, the Biome-BGC model exhibited less favorable performance in ET simulations in forest types before parameter optimization, compared to crops. However, the results became similar to those for GPP simulations after model parameter optimization. The values of R^2 increased for all vegetation cover types and values of RMSE decreased to varying degrees, resulting in an overall improvement in model performance for ET simulations (Table 2).

The simulation results for ET were similar to those for GPP. The Taylor diagrams showed noticeable differences in the distributions of data points before and after model parameter optimization. However, the distributions of ET data points were more concentrated than the GPP data points. Before optimization, the R^2 values for different vegetation types ranged from 0.2 to 0.7, and the RMSE values ranged from 15 to 60 mm. After parameter optimization, the R^2 values concentrated between 0.7 and 0.9, and the RMSE decreased to 5–30 mm. This indicates that parameter adjustment effectively reduced errors, making the simulated ET closer to the observed values. Through model parameter optimization, the improvement of simulation performance was the most obvious in the deciduous broad-leaved forest (Fig. 12a) and shrub meadow (Fig. 12c) regions. Additionally, simulation performance was the best in regions with annual crop (Fig. 12d) and wheat-paddy rotation (Fig. 12f). Vegetation distribution and underlying surface conditions had relatively smaller impacts on ET simulations than on GPP simulations. This is because the ET process has a more direct connection with environmental factors (such as temperature and humidity), while GPP is more sensitive to the unique physiological characteristics of vegetation, which vary significantly among different types. Therefore, the Taylor diagram

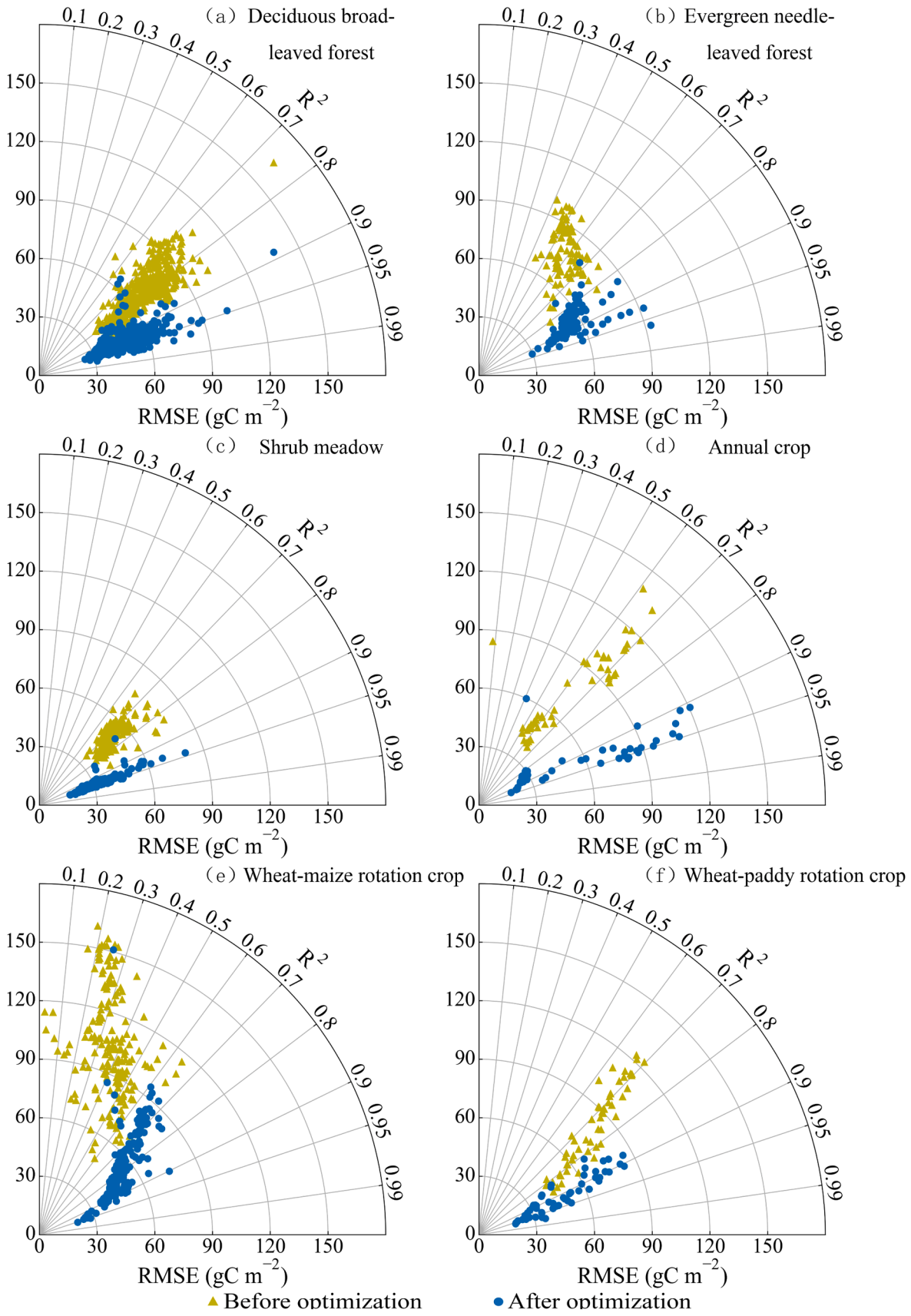

Fig. 10. Taylor plots of R^2 and RMSE distributions of observed and simulated GPP_{month} with the Biome-BGC model before (green triangles) and after (blue dots) optimization parameter under different typical vegetation types (deciduous broad-leaved forest, a; evergreen needle-leaved forest, b; shrub meadow, c; annual crop, d; wheat-maize rotation, e; and wheat-paddy rotation, f) in the Qinling Mountains of China.

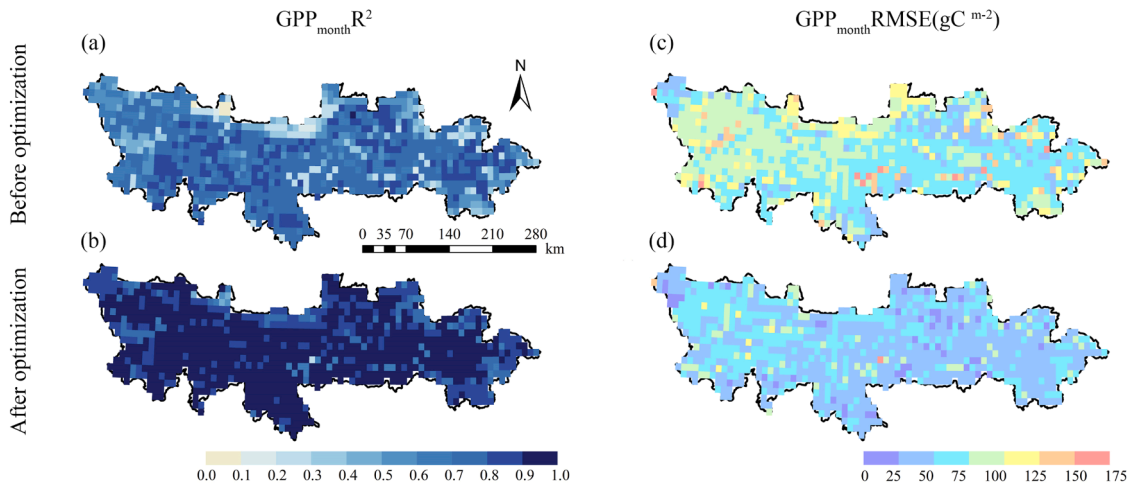

Fig. 11. Spatial distributions of R^2 (a, b) and RMSE (c, d) values between observed and simulated GPP_{month} with the Biome-BGC model before (a, c) and after (b, d) parameter optimization in the Qinling Mountains of China.

Table 2
Statistics of R^2, RMSE and MBE between simulated and observed ET_{month} before and after optimization of the Biome-BGC model parameters under different vegetation cover types of the Qinling Mountains of China.

Vegetation type	Before parameter optimization			After parameter optimization		
	R^2	RMSE (mm)	MBE (mm)	R^2	RMSE (mm)	MBE (mm)
Deciduous broad-leaved forest	0.61	38.31	15.22	0.89	14.65	−6.48
Evergreen needle-leaved forest	0.45	39.51	6.35	0.74	20.2	−4.21
Shrub meadow	0.45	41.74	20.44	0.89	16.93	0.01
Annual crop	0.78	16.61	−2.92	0.88	14.66	−0.53
Wheat-maize rotation crop	0.5	29.36	−25.41	0.83	16.31	−6.35
Wheat-paddy rotation crop	0.84	14.88	−4.16	0.91	11.43	−2.12
The Qinling Mountains	0.57	34.94	3.67	0.86	15.72	−1.98

quantifies this difference.

The R^2 and RMSE values of ET simulation results in the Qinling Mountains indicated that after parameter optimization, the overall R^2 values improved from 0.4–0.6 to 0.8–1.0, and RMSE values decreased from 30–50 mm to 10–20 mm, demonstrating a dramatic enhancement in simulation performance (Fig. 13). Before model parameter optimization, only the southwestern part of the Qinling Mountains exhibited higher R^2 values, while differences in other regions were less pronounced, all with low R^2 values. RMSE values followed an uneven distribution across the entire region of the Qinling Mountains. Through parameter optimization, the ET simulation performance was obviously improved, and the distributions of R^2 and RMSE of ET simulations became more uniform than those of GPP simulations. Meanwhile, the MBE results indicate that before parameter optimization, the ET simulation results for farmland ecosystems among vegetation cover types were lower than the actual values, while the simulation results for forest ecosystems, including deciduous broad-leaved forest, evergreen needle-leaved forest, and shrub meadow, overestimated ET. After model parameter optimization, the MBE values of the simulation results under different vegetation cover types are closer to 0.

4. Discussion

In this study, the PEST software was used to automatically estimate the parameters of the Biome-BGC model, thereby improving the efficiency of model parameter optimization. The PEST algorithm obtains optimization results through multiple iterations of the initial parameter vector. However, PEST involves many steps and is very complex to use, which increases the difficulties for model users (Song et al., 2015; Sun et al., 2014). This study integrated the PEST software with the Biome-BGC model to create a Python-based package of Biome-BGC-PEST, addressing the challenges of model parameter tuning faced for most model users. The program code of the Biome-BGC-PEST package was provided in the supplementary file.

In some previous studies, optimization of model genetic parameters with PEST often selected a set of default parameters based on user experience and parameter range adjustment in each iteration to achieve optimal parameter values (Song et al., 2015). However, this approach was susceptible to getting stuck in local optima, and the manual adjustment of parameter ranges before rerunning PEST was time-consuming and cumbersome, making it less user-friendly. If the initial parameter value vector was not selected rationally, satisfactory optimization results could not be obtained. Additionally, for new model users, it could also be very challenging for them to determine a vector of appropriate initial parameters. To address this issue, this study utilized multiple initial parameter sets, then conducted optimizations based on these parameter sets, and finally selected the best result from the multiple optimization outcomes. The test results showed that with the Biome-BGC-PEST package, the parameter sensitivity analysis and automatic optimization process could be completed within 30 min for a single site with more than 10 years of observation data, which was far more efficient than the manual parameter tuning process (Supplementary code). This improvement alleviated the problem of getting trapped in local optima encountered by the PEST software.

Then, this study conducted sensitivity analysis and optimization for the parameters of the Biome-BGC model with the newly established Biome-BGC-PEST package in the Qinling Mountains of China. The study identified the influential parameters both for GPP and ET simulations under typical vegetation cover types in the region. These influential parameters included: “atmospheric deposition of N”, “symbiotic and asymbiotic fixation of N”, “cuticular conductance”, “maximum stomatal conductance”, and etc. The types of influential parameters identified in this study were similar to several previous studies (Li and Sun, 2018; Li et al., 2018). It was found that the parameters of “C:N of leaves” and “Canopy water interception coefficient” were influential in both this present study and previous studies. This was primarily because changes in “C:N of leaves” could affect the nitrogen content of ribulose-1, 5-bisphosphate carboxylase/oxygenase, thereby influence photosynthesis (White et al., 2000). The canopy water interception coefficient

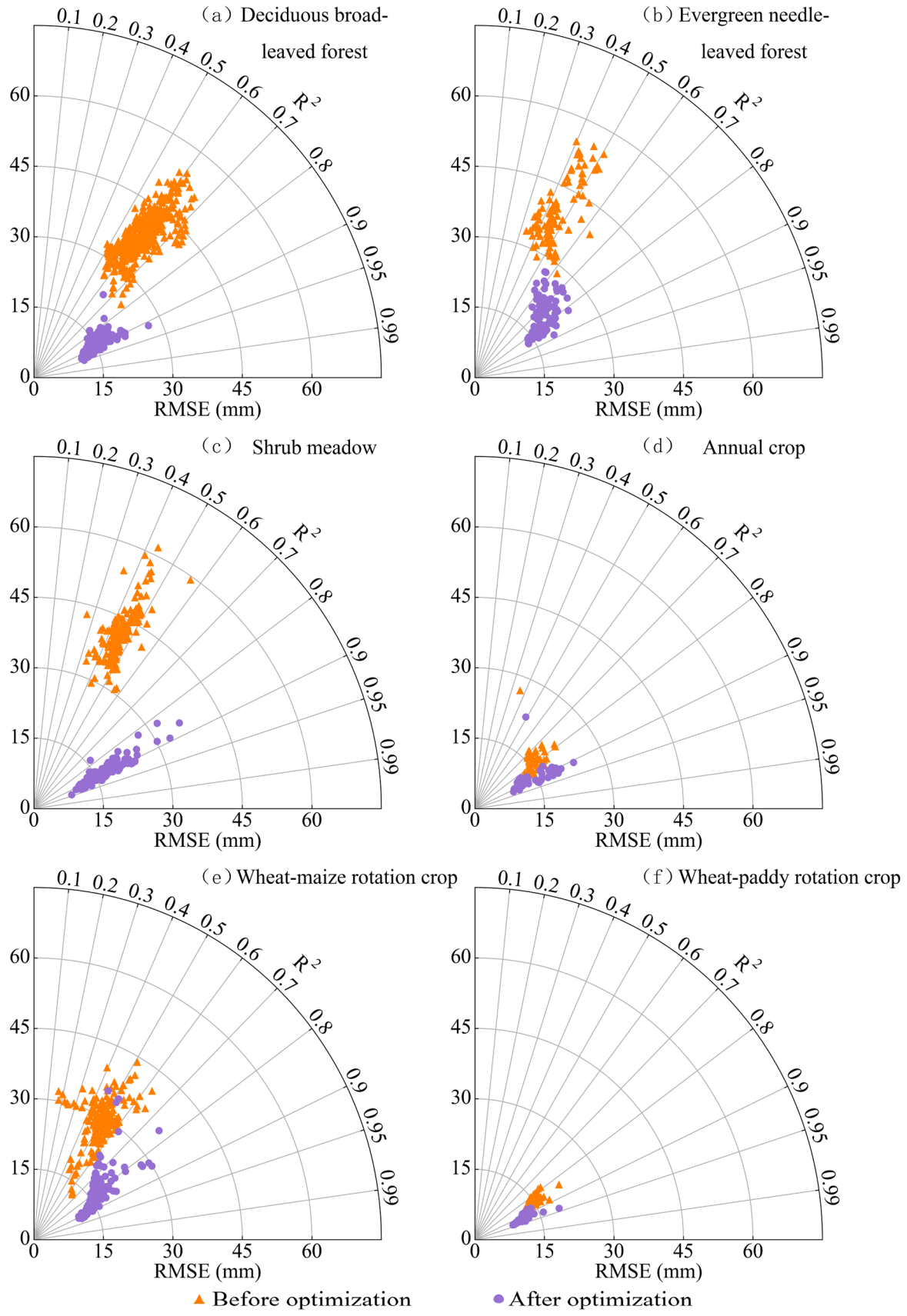

Fig. 12. Taylor plots of R^2 and RMSE distributions of observed and simulated ET_{month} with the Biome-BGC model before and after parameter optimization under different typical vegetation cover types (deciduous broad-leaved forest, a; evergreen needle-leaved forest, b; shrub meadow, c; annual crop, d; wheat-maize rotation, e; and wheat-paddy rotation, f) in the Qinling Mountains of China.

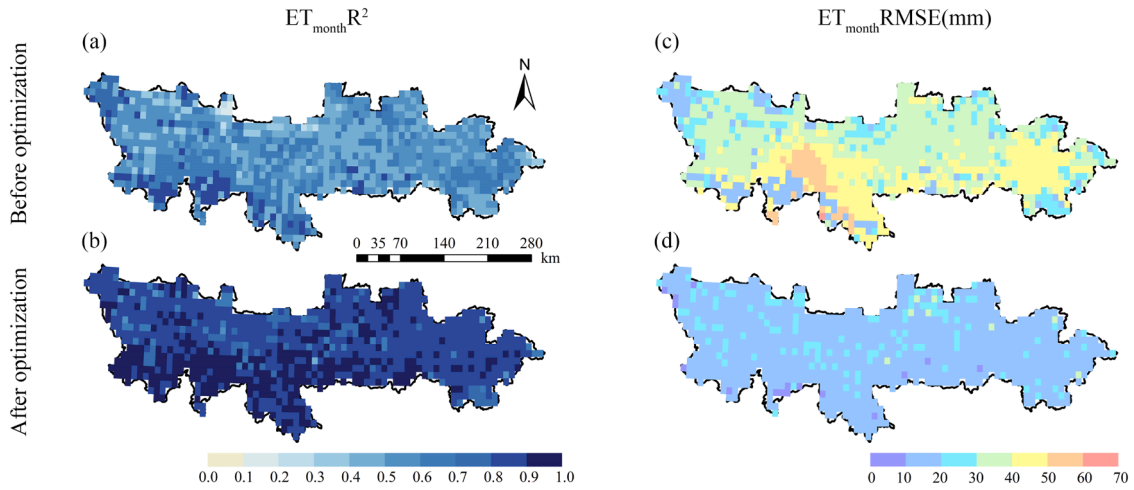

Fig. 13. Spatial distributions of R^2 (a, b) and RMSE (c, d) values between observed and simulated ET_{month} with the Biome-BGC model before (a, c) and after (b, d) parameter optimization in the Qinling Mountains of China.

could determine the amount of precipitation intercepted by the canopy and control the volume of precipitation infiltrating into the soil. An increase of this coefficient indicated a more closed canopy with increased interception, reduced throughfall within the forest, and correspondingly decreased soil water sources to some extent, which in turn could affect the simulations of GPP and ET.

Additionally, this study found that the GPP and ET simulations of the Biome-BGC model were highly sensitive to the parameters of "Annual leaf and fine root turnover fraction" for evergreen needle-leaved forest and shrub meadow of the forest ecosystems, while such sensitivity was not significant for the farmland ecosystems (Table S5). This was mainly because the growth, senescence, and turnover processes of leaves in evergreen needle-leaved forest were relatively slow but occurred continuously, so these parameters could affect the efficiency of plants in absorbing and utilizing nutrients. For shrub meadow, their root systems were shallowly distributed with a high proportion of fine roots and the turnover rate of fine roots was relatively fast, which could partially explain the influences of these parameters. Furthermore, the GPP and ET simulations of tree-dominated vegetation types (i.e., evergreen needle-leaved forest and deciduous broad-leaved forest) were sensitive to the parameter of "Annual live wood turnover fraction". This was primarily because live xylem constituted the core structural and functional unit of trees and served as the main reservoir for carbon storage in trees, thus directly affecting the growth efficiency of trees. Furthermore, for the differences in the magnitudes of parameter sensitivity between this study and previous researches, the main reason was probably because earlier studies often focused on the sensitivity of individual parameters for carbon and water flux simulations, without considering the interactions among different model parameters.

The Qinling Mountains act as a natural divider between northern and southern China, rich in forest resources and offering substantial carbon sequestration potentials (Chen, 2019). Moreover, they play a pivotal role as a primary water source for the Central Route of the South-to-North Water Diversion Project of China, contributing about 70 % of the total water volume diverted (Bai and Li, 2022). The significance of the Qinling Mountains as water resources for the socioeconomic development of North China has been growing, currently easing water scarcity issues in Beijing, the capital of China (Wang et al., 2023a). The Biome-BGC model, which was calibrated with the Biome-BGC-PEST package, enables more precise simulations of GPP and ET in the Qinling Mountains. This will greatly facilitate quantifying the contributions of the ecosystems of the Qinling Mountains to climate regulation, soil and water conservation, water resource retention, and carbon sequestration in China. The Biome-BGC-PEST package developed in this study can also be applied to other regions and similar ecosystems since it only relies on the model input variables and model validation data of the study area. Furthermore, the application of this package could dramatically improve the efficiency of model calibration, thereby facilitating model simulations at large regional scales.

5. Conclusions

This study coupled the Biome-BGC model with the parameter optimization program of PEST using Python language to greatly simplify the processes of model parameter estimation and enable automatic model optimization. Then, this study validated the Biome-BGC-PEST package to optimize the influential parameters of the Biome-BGC model for different vegetation cover types in the Qinling Mountains of China. The main conclusions were drawn as follows.

(1) The newly developed Biome-BGC-PEST package for automatic model parameter optimization could dramatically streamline the processes and steps of parameter optimization for the Biome-BGC model. Hence, this study provided a useful reference for the optimization of other ecological models with the PEST software.
(2) The influential parameters of the Biome-BGC model were obtained through parameter sensitivity analysis for GPP and ET simulations under different typical vegetation cover types in the Qinling Mountains, which included "atmospheric deposition of N", "symbiotic and asymbiotic fixation of N", "cuticular conductance", "maximum stomatal conductance", and etc.
(3) After parameter optimization, the Biome-BGC model was able to simulate the GPP and ET fluxes in the Qinling Mountains with obviously improved simulation performance. For GPP, the general R^2 between observed and simulated values increased from 0.67 to 0.89, and the general RMSE decreased from 75.99 gC m^{-2} to 47.86 gC m^{-2}. For ET, the general R^2 between observed and simulated values improved from 0.57 to 0.86, and the general RMSE decreased from 34.94 mm to 15.72 mm.

Based on the new findings of this study, it was proposed that future research could further integrate farmland management practices into the model simulations and test the adaptability of this package under extreme environmental conditions. This would contribute to ecosystem management and assist in addressing the challenges posed by climate change in the Qinling Mountains of China.

CRediT authorship contribution statement

Kaiyuan Gong: Writing – original draft, Validation, Software, Methodology, Investigation, Formal analysis. **Zhuo Huang:** Writing – review & editing, Software, Methodology, Investigation. **Linsen Wu:** Data curation. **Zhihao He:** Supervision, Methodology. **Junqing Chen:** Methodology. **Zhao Wang:** Funding acquisition. **Qiang Yu:** Supervision, Methodology. **Hao Feng:** Writing – review & editing. **Jianqiang He:** Writing – review & editing, Supervision, Methodology, Funding acquisition.

Declaration of competing interest

The authors declare that they have no known competing financial interests or personal relationships that could have appeared to influence the work reported in this paper.

Acknowledgments

This research was partially supported by the National Natural Science Foundation of China (No. 52579046), the National Key Research and Development Program of China (No. 2021YFD1900700), the Qinling Ecological Protection Project 2023 by the Development and Reform Commission of Shaanxi Province: '*Study on weather and climate characteristics and eco-environmental evolutions in the Qinling Mountains*', and the "111 Project" (No. B12007) of China.

Supplementary materials

Supplementary material associated with this article can be found, in the online version, at doi:10.1016/j.agrformet.2025.110868.

Data availability

Data will be made available on request.

References

Bahremand, A., De Smedt, F., 2010. Predictive analysis and simulation uncertainty of a distributed hydrological model. Water Resour. Manag. 24, 2869–2880. https://doi.org/10.1007/s11269-010-9584-1.

Bai, R., Li, J., 2022. Research on institutional guarantee of ecological compensation mechanism for water source area of the middle route project of the south-to-North water transfer: taking the three cities of Southern Shaanxi in Qinling Area as examples. Ecol. Econ. 209–214, 1671-4407(2022)11-209-06 (in Chinese).

Baldocchi, D., 1994. A comparative study of mass and energy exchange rates over a closed C3 (wheat) and an open C4 (corn) crop: II. CO2 exchange and water use efficiency. Agric. For. Meteorol. 67, 291–321. https://doi.org/10.1016/0168-1923(94)90008-6.

Beer, C., Ciais, P., Reichstein, M., Baldocchi, D., Law, B.E., Papale, D., Soussana, J.F., Ammann, C., Buchmann, N., Frank, D., 2009. Temporal and among-site variability of inherent water use efficiency at the ecosystem level. Glob. Biogeochem. Cycles. 23. https://doi.org/10.1029/2008GB003233.

Beer, C., Reichstein, M., Tomelleri, E., Ciais, P., Jung, M., Carvalhais, N., Rödenbeck, C., Arain, M.A., Baldocchi, D., Bonan, G.B., 2010. Terrestrial gross carbon dioxide uptake: global distribution and covariation with climate. Science (1979) 329, 834–838. https://doi.org/10.1126/science.1184984.

Bezak, N., Rusjan, S., Petan, S., Sodnik, J., Mikoš, M., 2015. Estimation of soil loss by the WATEM/SEDEM model using an automatic parameter estimation procedure. Environ. Earth. Sci. 74, 5245–5261. https://doi.org/10.1007/s12665-015-4534-0.

Bond-Lamberty, B., Gower, S.T., Ahl, D.E., 2007. Improved simulation of poorly drained forests using Biome-BGC. Tree Physiol. 27, 703–715. https://doi.org/10.1093/treephys/27.5.703.

Chen, Y., 2019. Significance and strategies on the ecological civilization construction at Qinling Mountains. J. Earth Environ. 10, 1–11. https://doi.org/10.7515/JEE182056 in Chinese.

Chen, Y., Xiao, W., 2019. Estimation of forest NPP and carbon sequestration in the Three Gorges Reservoir Area, using the biome-BGC model. Forests. 10, 149. https://doi.org/10.3390/f10020149.

Chiesi, M., Maselli, F., Moriondo, M., Fibbi, L., Bindi, M., Running, S.W., 2007. Application of BIOME-BGC to simulate Mediterranean forest processes. Ecol. Modell. 206, 179–190. https://doi.org/10.1016/j.ecolmodel.2007.03.032.

Ciais, P., Sabine, C.L., Bala, G., Bopp, L., Brovkin, V.A., Canadell, J.G., Chhabra, A., DeFries, R.S., Galloway, J.N., Heimann, M., Jones, C.D., Le Qu, E R EC., Myneni, R. B., Piao, S., Thornton, P.E., 2014. Climate Change 2013 – The Physical Science Basis: Working Group I Contribution to the Fifth Assessment Report of the Intergovernmental Panel on Climate Change. Cambridge University Press, Cambridge.

Doherty, J., Brebber, L., Whyte, P., PEST: model-independent parameter estimation. Watermark Comput., Corinda, Australia. 122, 336.

Fang, Q., Green, T.R., Ma, L., Erskine, R.H., Malone, R.W., Ahuja, L.R., 2010. Optimizing soil hydraulic parameters in RZWQM2 under fallow conditions. Soil Sci. Soc. Am. J. 74, 1897–1913. https://doi.org/10.2136/sssaj2009.0380.

Fang, Q., Malone, R., Ma, L., Jaynes, D., Thorp, K., Green, T., Ahuja, L., 2012. Modeling the effects of controlled drainage, N rate and weather on nitrate loss to subsurface drainage. Agric. Water. Manag. 103, 150–161. https://doi.org/10.1016/j.agwat.2011.11.006.

Farr, T.G., Kobrick, M., 2000. Shuttle radar topography mission produces a wealth of data. Eos, Trans. Am. Geophys. Union. 81, 583–585. https://doi.org/10.1029/EO081i048p00583.

Friedel, M.J., 2005. Coupled inverse modeling of vadose zone water, heat, and solute transport: calibration constraints, parameter nonuniqueness, and predictive uncertainty. J. Hydrol. 312, 148–175. https://doi.org/10.1016/j.jhydrol.2005.02.013.

Gao, W., Zhou, F., Dong, Y., Guo, H., Peng, J., Xu, P., Zhao, L., 2014. PEST-based multi-objective automatic calibration of hydrologic parameters for HSPF model. J. Nat. Resour. 29, 855–867. https://doi.org/10.11849/zrzyxb.2014.05.013 in Chinese.

Hengl, T., de Jesus, J.M., MacMillan, R.A., Batjes, N.H., Heuvelink, G.B.M., Ribeiro, E., Samuel-Rosa, A., Kempen, B., Leenaars, J.G.B., Walsh, M.G., Gonzalez, M.R., 2014. SoilGrids1km — Global soil information based on automated mapping. PLoS. One 9, e105992. https://doi.org/10.1371/journal.pone.0105992.

Huang, X., Chen, C., Yao, B., Ma, Z., Zhou, H., 2022a. Spatiotemporal dynamics of the carbon budget and the response to grazing in Qinghai grasslands. Front. Plant Sci. 12. - 2021.

Huang, Z., Cao, Y., Xu, X., Chen, S., Feng, H., Wang, Z., Yu, Q., He, J., 2022b. Study on the ecosystem water use efficiency of the Qinling Mountains with multi-source GPP and ET products. J. Soil. Water. Conserv. 36, 181–194. https://doi.org/10.13870/j.cnki.stbcxb.2022.05.024, 203in Chinese.

Jia, L., Zhang, B., 2024. Simulating the vegetation gross primary productivity by the biome-BGC model in the Yellow River Basin of China. Water. (Basel) 16. https://doi.org/10.3390/w16233468.

Kumar, M., Raghubanshi, A., 2012. Sensitivity analysis of BIOME-BGC model for dry tropical forests of Vindhyan highlands, India. Int. Arch. Photogramm., Rem. Sens. Spat. Inf. Sci. 38, 129–133. https://doi.org/10.5194/isprsarchives-XXXVIII-8-W20-129-2011.

Li, C., Sun, H., Wu, X., Han, H., 2020. An approach for improving soil water content for modeling net primary production on the Qinghai-Tibetan Plateau using Biome-BGC model. Catena (Amst) 184, 104253. https://doi.org/10.1016/j.catena.2019.104253.

Li, X., Sun, J., 2018. Testing parameter sensitivities and uncertainty analysis of biome-BGC model in simulating carbon and water fluxes in broadleaved-Korean pine forests. Chin. J. Plant Ecol. 42, 1131–1144. https://doi.org/10.17521/cjpe.2018.0231 in Chinese.

Li, Y.Z., Zhang, T.L., Liu, Q.Y., Li, Y., 2018. Temporal and spatial heterogeneity analysis of optimal value of sensitive parameters in ecological process model: the BIOME-BGC model as an example. J. Appl. Ecol. 29, 84–92. https://doi.org/10.13287/j.1001-9332.201801.016 in Chinese.

Liu, H., Ding, Q., Li, Y., Fan, L., Zhao, L., Ma, M., 2025. Improved biome-BGC model for simulating spatiotemporal dynamics of gross primary productivity in evergreen broadleaf forests of the karst region. Environ. Model. Softw. 192, 106563. https://doi.org/10.1016/j.envsoft.2025.106563.

Liu, M., Wu, Z., 2012. Review of hydrologic cycle of forest ecosystem. Trop. Agric. Eng. 36, 13–20. CNKI:SUN:RDZW.0.2012-01-005in Chinese.

Ma, H., Malone, R.W., Jiang, T., Yao, N., Chen, S., Song, L., Feng, H., Yu, Q., He, J., 2020. Estimating crop genetic parameters for DSSAT with modified PEST software. Euro. J. Agron. 115, 126017. https://doi.org/10.1016/j.eja.2020.126017.

Ma, L., Ahuja, L., Nolan, B., Malone, R., Trout, T., Qi, Z., 2012. Root zone water quality model (RZWQM2): model use, calibration, and validation. Trans. ASABe 55, 1425–1446. https://doi.org/10.13031/2013.42252.

Malone, R., Jaynes, D., Ma, L., Nolan, B., Meek, D., Karlen, D., 2010. Soil-test N recommendations augmented with PEST-optimized RZWQM simulations. J. Environ. Qual. 39, 1711–1723. https://doi.org/10.2134/JEQ2009.0425.

Nolan, B.T., Puckett, L.J., Ma, L., Green, C.T., Bayless, E.R., Malone, R.W., 2010. Predicting unsaturated zone nitrogen mass balances in agricultural settings of the United States. J. Environ. Qual. 39, 1051–1065. https://doi.org/10.2134/jeq2009.0310.

Pan, Y., Birdsey, R.A., Fang, J., Houghton, R., Kauppi, P.E., Kurz, W.A., Phillips, O.L., Shvidenko, A., Lewis, S.L., Canadell, J.G., 2011. A large and persistent carbon sink in the world's forests. Science (1979) 333, 988–993. https://doi.org/10.1126/science.1201609.

Priestley, C.H.B., Taylor, R.J., 1972. On the assessment of surface heat flux and evaporation using large-scale parameters. Mon. Weather. Rev. 100, 81–92. https://doi.org/10.1175/1520-0493(1972)100<0081:OTAOSH>2.3.CO;2.

Raj, R., Hamm, N.A., van der Tol, C., Stein, A., 2014. Variance-based sensitivity analysis of BIOME-BGC for gross and net primary production. Ecol. Modell. 292, 26–36. https://doi.org/10.1016/j.ecolmodel.2014.08.012.

Ren, H., Zhang, L., Yan, M., Tian, X., Zheng, X., 2022. Sensitivity analysis of biome-BGCMuSo for gross and net primary productivity of typical forests in China. For. Ecosyst. 9, 100011. https://doi.org/10.1016/j.fecs.2022.100011.

Running, S.W., Hunt Jr, E.R., 1993. Generalization of a forest ecosystem process model for other biomes, BIOME-BCG, and an application for global-scale models. Scaling

physiological processes: leaf to globe. https://doi.org/10.1016/B978-0-12-233440-5.50014-2.
Running, S.W., Nemani, R.R., Hungerford, R.D., 1987. Extrapolation of synoptic meteorological data in mountainous terrain and its use for simulating forest evapotranspiration and photosynthesis. Can. J. For. Res. 17, 472–483. https://doi.org/10.1139/x87-081.
Ryu, Y., Baldocchi, D.D., Kobayashi, H., Van Ingen, C., Li, J., Black, T.A., Beringer, J., Van Gorsel, E., Knohl, A., Law, B.E., 2011. Integration of MODIS land and atmosphere products with a coupled-process model to estimate gross primary productivity and evapotranspiration from 1 km to global scales. Global. Biogeochem. Cycles. 25. https://doi.org/10.1029/2011GB004053.
Skahill, B.E., Doherty, J., 2006. Efficient accommodation of local minima in watershed model calibration. J. Hydrol. 329, 122–139. https://doi.org/10.1016/j.jhydrol.2006.02.005.
Song, L., Chen, S., Yao, N., Feng, H., Zhang, T., He, J., 2015. Parameter estimation and verification of CERES-maize model with GLUE and PEST methods. Trans. Chin. Soc. Agric. Mach. 46, 95–111. https://doi.org/10.6041/j.issn.1000-1298.2015.11.015.
Sun, M., Zhang, X., Feng, S., Huo, Z., 2014. Parameter optimization and validation for RZWQM2 model using PEST method. Trans. Chin. Soc. Agric. Mach. 45, 146–153. https://doi.org/10.6041/j.issn.1000-1298.2014.11.023 in Chinese.
Sun, Q., Li, B., Zhang, T., Yuan, Y., Gao, X., Ge, J., Li, F., Zhang, Z., 2017. An improved biome-BGC model for estimating net primary productivity of alpine meadow on the Qinghai-Tibet Plateau. Ecol. Modell. 350, 55–68. https://doi.org/10.1016/j.ecolmodel.2017.01.025.
Tebakari, T., Kita, R., 2015. Estimating permeability using the parameter estimation method in a high-permeability area of the Kurobe River alluvial Fan, Japan. Procedia Environ. Sci. 25, 235–242. https://doi.org/10.1016/j.proenv.2015.04.032.
Ueyama, M., Ichii, K., Hirata, R., Takagi, K., Asanuma, J., Machimura, T., Nakai, Y., Ohta, T., Saigusa, N., Takahashi, Y., 2010. Simulating carbon and water cycles of larch forests in East Asia by the BIOME-BGC model with AsiaFlux data. Biogeosciences. 7, 959–977. https://doi.org/10.5194/bg-7-959-2010.
Wang, Q., Watanabe, M., Ouyang, Z., 2005. Simulation of water and carbon fluxes using BIOME-BGC model over crops in China. Agric. For. Meteorol. 131, 209–224. https://doi.org/10.1016/j.agrformet.2005.06.002.
Wang, K., Wei, R., Qi, S., Yao, J., Xinhan, X., Yi, W., Yiping, C., 2023a. Progress in research and practice of ecological compensation theory in the Qinling Mountains. J. Earth Environ. 14, 263–271. https://doi.org/10.7515/JEE221012 in Chinese.
Wang, T., Bai, H., 2017. Variation of vegetation NDVI in response to climate changes and human activities in Qinling mountains. Mountain Res. 35, 778–789. https://doi.org/10.16089/j.cnki.1008-2786.000278 in Chinese.
Wang, Y., Zhou, H., Huang, J., Yu, J., Yuan, Y., 2023b. A framework for identifying propagation from meteorological to ecological drought events. J. Hydrol. 625, 130–142. https://doi.org/10.1016/j.jhydrol.2023.130142.
White, M.A., Thornton, P.E., Running, S.W., Nemani, R.R., 2000. Parameterization and sensitivity analysis of the BIOME–BGC terrestrial ecosystem model: net primary production controls. Earth. Interact. 4, 1–85. https://doi.org/10.1175/1087-3562(2000)004<0003:PASAOT>2.0.CO;2.
Xia, Y., Fu, C., Wu, H., Wu, H., Zhang, H., Cao, Y., Zhu, Z., 2021. Influences of extreme events on water and carbon cycles of cropland ecosystems: a comprehensive exploration combining site and global modeling. Water. Resour. Res. 57, e2021WR029884. https://doi.org/10.1029/2021WR029884.
Yan, M., Tian, X., Li, Z., Chen, E., Wang, X., Han, Z., Sun, H., 2016. Simulation of forest carbon fluxes using model incorporation and data assimilation. Rem. Sens. (Basel) 8, 567. https://doi.org/10.3390/rs8070567.
You, Y., Wang, S., Ma, Y., Wang, X., Liu, W., 2019. Improved modeling of gross primary productivity of alpine grasslands on the Tibetan plateau using the biome-BGC model. Rem. Sens. (Basel) 11. https://doi.org/10.3390/rs11111287.
Yu, R., Yao, Y., Tang, Q., Shao, C., Fisher, J.B., Chen, J., Jia, K., Zhang, X., Li, Y., Shang, K., 2023. Coupling a light use efficiency model with a machine learning-based water constraint for predicting grassland gross primary production. Agric. For. Meteorol. 341, 109634. https://doi.org/10.1016/j.agrformet.2023.109634.
Zhen, X., Huo, W., Tian, D., Zhang, Q., Sanz-Saez, A., Chen, C.Y., Batchelor, W.D., 2023. County level calibration strategy to evaluate peanut irrigation water use under different climate change scenarios. Euro. J. Agron. 143, 126693. https://doi.org/10.1016/j.eja.2022.126693.